

## **Coupled processes during rainfall: an experimental investigation on a silty sand**

F. Casini<sup>1</sup>

<sup>1</sup> Marie Curie Intra-European Fellow, Departamento de Ingeniería del Terreno, Cartográfica y Geofísica, C.JORDI GIRONA 1-3, Universitat Politècnica de Catalunya; 08034 Barcelona, Spain, email: [francesca.casini@upc.edu](mailto:francesca.casini@upc.edu)

### **ABSTRACT**

The factors that contributed to the initiation of a triggering mechanism in a shallow landslides induced by rainfall are investigated in this work at laboratory scale. The aim of the work was to characterise the behaviour of the soil in triaxial tests, in the light of the possible failure mechanisms in a slope subjected to rainfall. The material study is a silty sand from a steep slope in Ruedlingen in the North-East of Switzerland, where a landslide triggering experiment was carried out. Conventional drained and undrained triaxial tests for the water phase were conducted to detect critical state conditions as well as peak shear strength as a function of confining pressure for three different water content related to the in situ one. Soil specimens with three different gravimetric water contents were exposed to stress paths simulating the in situ anisotropic compression followed by a decrease of mean effective stress at constant axial load. Possible unstable response along the stress paths analysed was investigated by means of second order work.

### **INTRODUCTION**

Mountainous areas tend to be exposed to an enhanced risk of damage caused by natural hazards. In addition to general risks such as earthquakes and storms, risks are exacerbated by the topography (leading to gravitational mass movements such as avalanches, mud and debris flows). Six percent of the area of Switzerland is prone to slope instability (Springman et al 2012).

The influence of rainfall events on slope stability was studied by instrumenting a natural slope in Ruedlingen, Switzerland, and subjecting it to a series of artificial rainfall events (Askarinejad et al 2012). The project was designed to replicate the effects of a heavy rainfall event in May 2002, in which 100 mm rain fell in 40 minutes (Fischer et al. 2003), causing 42 surficial landslides in the locality. To understand the hydro-mechanical conditions leading to initiation of failure mechanisms better, an extensive experimental investigation was planned to encompass both saturated and unsaturated conditions. The results of the unsaturated and saturated statically compacted specimens tested under triaxial stress conditions will be discussed herein (Casini *et al* 2013).

The compressibility behaviour has been analysed using a Bishop stress approach (Bishop 1959), and a simple equation is proposed to model the results based on the Modified Cam Clay Model (MCCM), which depends on the stress ratio, the effective stress parameter  $\chi$ , and a parameter  $a$ , which controls the rate of change of the

preconsolidation pressure induced by change in parameter  $\chi$ . The occurrence of instability during the shearing phase has been explored by means of Hill's sufficient condition of stability (Hill 1958), which is based on the sign of the second-order work. The results are interpreted within a unified framework proposed by Chu et al. (2003), which has been extended to unsaturated conditions with the aim of providing a useful model for the response.

## **EXPERIMENTAL PROGRAMME**

The specimens have been prepared by static compaction, in order to reproduce mean values of dry density and water content expected under natural unsaturated in situ conditions. The reconstituted specimens were then prepared by static compaction with a gravimetric water content  $w_0=0.17$  and  $e_0=0.95$  and were tested in three modes: 1) as compacted, 2) by increasing the water content to  $w_1=0.25$  and 3) to  $w=w_{\text{sat}}$ , by infiltrating water from the bottom of the specimen.

The main objectives of the experimental programme were to characterise the behaviour under unsaturated and saturated conditions and to investigate the potential for instability of the Ruedlingen soil during shearing to failure. Conventional stress path tests were performed on specimens with three gravimetric water contents, as mentioned above, as well as on paths approaching those experienced in the field.

The soil is unsaturated under in situ conditions. The gravimetric water content range derived from monitoring was between 0.17-0.25 to completely saturated, depending on the season. The following stress paths are investigated to represent the response of the soil in the slope: CIUC: isotropic consolidation - standard undrained compression for the saturated specimens;  $\text{CIU}_w\text{C}$ : isotropic consolidation - undrained compression for the water phase for the specimens with  $w=0.17$  and 0.25; CADCAL: anisotropic consolidation - drained shear by decreasing mean effective stress pressure at constant axial load for saturated and unsaturated specimens.

The water retention properties for the Ruedlingen soil have been obtained on specimens that were compacted statically under suction controlled conditions to three different void ratios. A wetting path has been followed at three void ratios (Fig. 1), particular attention has been paid to the evolution of the wetting path dependent on the void ratios, because it is the typical path experienced under field conditions during a rainfall event. The evolution of the WRC with void ratio plays a fundamental role in the evaluation of the stability of steep slopes due to the coupling effects of suction and degree of saturation (Askarinejad *et al* 2011).

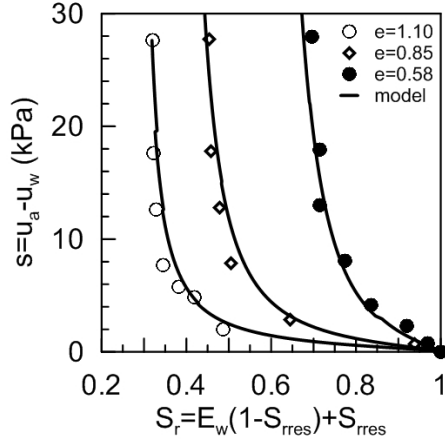


Figure 1. Water retention curves obtained under suction controlled conditions and model prediction

## EXPERIMENTAL RESULTS

### Modelling water retention properties

The wetting water storage mechanism has been described using a modified Van Genuchten (1980) model in terms of dimensionless water ratio  $E_w = E_w(s, n)$  as follows:

$$E_w = \frac{e_w - e_{wres}}{e - e_{wres}} = (1 + (s/P(n))^{1/1-\lambda(n)})^{-\lambda(n)}; \quad (1)$$

$$P(n) = P_0 e^{b(n_0 - n)}; \quad \lambda(n) = \lambda_0 e^{c(n_0 - n)}$$

where  $e_w = V_w/V_s = S_r e$ ,  $V_s$  is the volume of solids,  $e_{wres} = 0.30$  is the residual water ratio,  $P$ ,  $P_0$ ,  $\lambda_0$  and  $\lambda$  are soil parameters, depending on porosity  $n$  via parameters  $b$  and  $c$ . The parameters obtained by interpreting the WRC are reported in Casini *et al* 2013. Comparison between the prediction and the laboratory results for the WRC is shown in Fig. 1 in terms of  $S_r$  versus  $s$ . The model fits the experimental results well over the variation of void ratio and in the range of suction investigated.

### Triaxial tests and its modelling

#### Consolidation phase

The consolidation phase has been performed with a mean stress rate  $\dot{p} = 3.6$  kPa/h up to a mean total stress of  $p = 95$  kPa for four different obliquities  $\eta = q/p'$ . The suction has been evaluated through the Water Retention Curve by following the evolution of the degree of saturation during the test. The experimental results are reported in Fig. 2 for the same  $\eta$  and the different gravimetric water contents, in terms of void ratio  $e = V_v/V_s$  ( $V_s$  volume of solid particles) and mean skeleton stress  $p' = p - u_a + S_r(u_a - u_w)$ .

The mean soil skeleton (effective) stress is defined as  $p' = p - u_a + \chi(u_a - u_w)$  with  $\chi = S_r$ . Following the approach proposed by Casini (2012) in 1-D condition and extended by Casini *et al* (2013) to triaxial conditions the Normal Compression Line, for a given obliquity  $\eta = q/p'$ , is given by

$$v = N_\eta(\chi) - \lambda \ln p_{c\eta}' \quad N_\eta(\chi) = N_0(1) + (\lambda - \kappa) \left[ a(1 - \chi) + \ln\left(\frac{M^2}{M^2 + \eta^2}\right) \right]$$

where  $N_0(1)$  is the specific value at  $p'=1$  kPa for  $\eta=q/p'=0$ ,  $\lambda$  is the compressibility index and  $\kappa$  the unloading-reloading line in  $v$ - $\ln p'$  space,  $M$  the slope of critical state line,  $a$  a constitutive parameter (for more details see Casini 2012 and Casini *et al* 2013). The model fit well the experimental results over the obliquity and water content tested as reported in Figure 4.

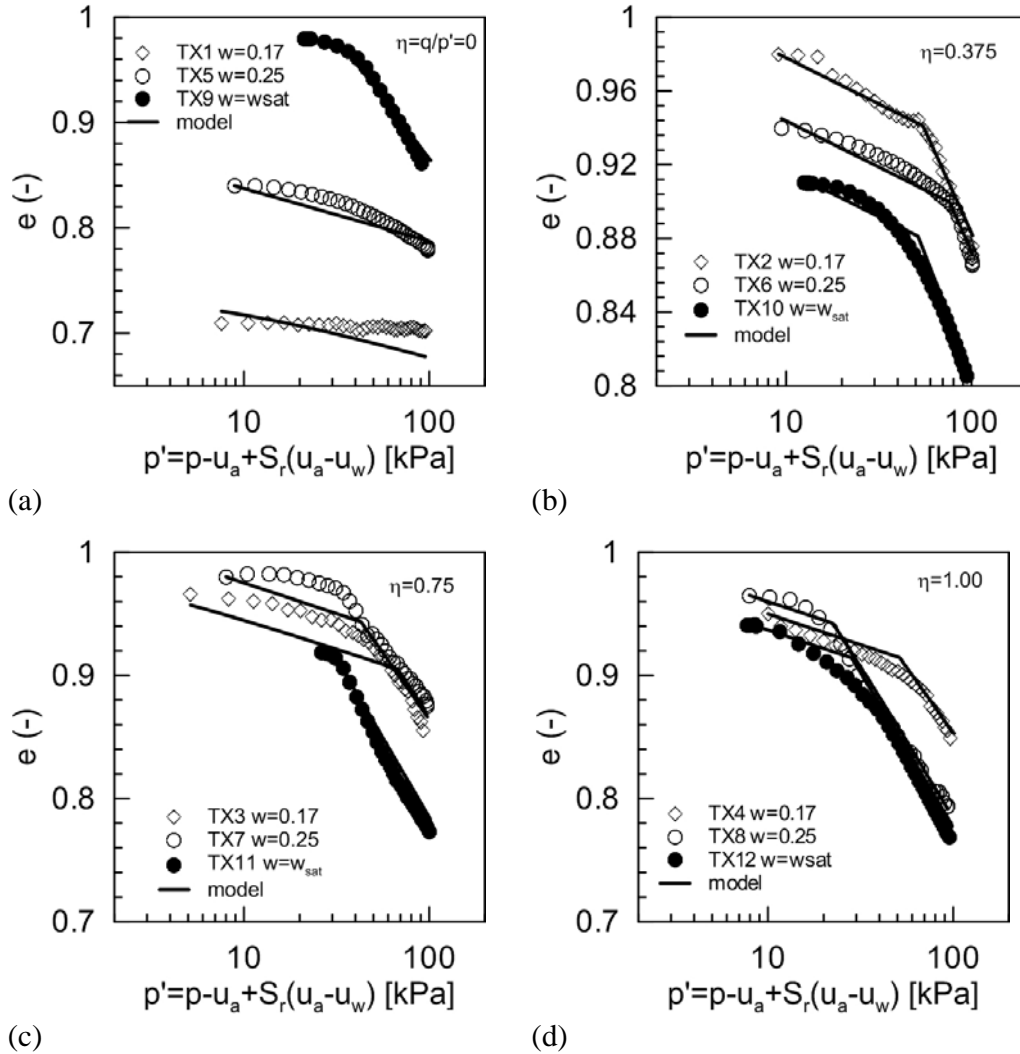


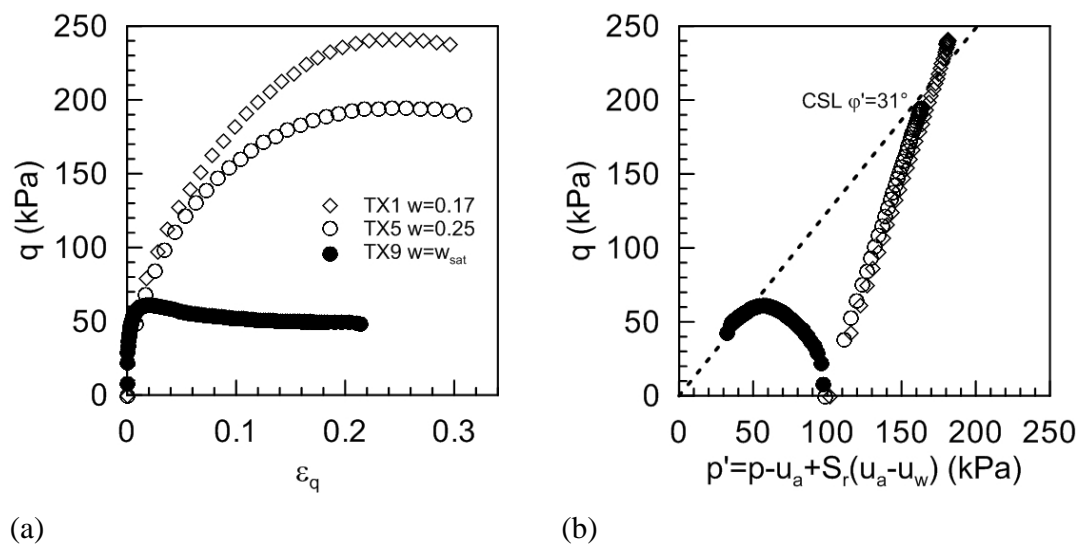
Figure 2. Comparison between model prediction and experimental data for the consolidation phase: (a)  $\eta=0$ ; (b)  $\eta=0.375$ ; (c)  $\eta=0.75$ ; (d)  $\eta=1.00$ .

### Compression phase

The results of the specimens compressed under a controlled displacement rate ( $5 \cdot 10^{-4}$  mm/s) are reported in Fig. 5 in the planes  $\epsilon_q$ - $q$ ,  $p'$ - $q$ ,  $\epsilon_q$ - $\epsilon_v$  and  $e$ - $\log(p')$  respectively.

The peak deviator  $q_{\text{peak}}$  increases with decreasing water content at the same confinement stress. The saturated specimen TX9 is sheared at constant volume (undrained; Fig. 5d) and shows a slightly brittle behaviour with  $q_{\text{peak}}=60$  kPa and a residual  $q_{\text{res}}=50$  kPa (Fig. 3a). The excess pore pressure  $\Delta u$  increases with  $\varepsilon_q$ , displaying typical behaviour of contractant soil (Fig. 3b & c). The unsaturated specimens (TX1 and TX5) exhibit an initial decrease in volume followed by dilatant behaviour. The dilatancy increases with lower water content (Fig. 3c & d). The behaviour observed is consistent with the position of the points representing the state of the specimens at the end of the consolidation phase (Fig. 2a), the saturated specimen TX9 is on the Normal Compression Line (NCL) at the end of the consolidation phase (expected contractant behaviour at failure), while specimens TX1 and TX5 are on an unloading-reloading line (expected dilatant behaviour at failure) with the specimen at  $w=0.17$  having the greatest overconsolidation ratio and hence potential for dilation. A value of  $\eta_{\text{CSL}}=M=1.24$  denotes the gradient of the Critical State Line (CSL), corresponding to a critical state friction angle of  $\phi'=31^\circ$ , and represents a good fit to the critical state conditions (Fig. 3b).

The measured degree of saturation  $S_r=e_w/e$ , and the predicted suction (via the WRC) during the axial compression phase, are reported in Fig. 5e for specimens TX1 and TX5 with the initial contractance clearly shown before dilatancy takes over at  $\varepsilon_q>0.1$ , leading to a reduced  $S_r$ . The  $S_r$ -s and  $E_w$ -s paths are also reported in Fig. 3f. The variation of  $S_r$  due to the change in void ratio ( $e_w=\text{constant}$ ) induces a more pronounced adjustment in suction for TX1 ( $w=0.17$ ), which is due to the different initial position on the WRC according to the model reported in Fig. 1. The point representative for  $S_{r0}=0.6$  (TX5) is near the lower bound corner of the WRC, so a small change in  $S_r$  provokes a significant change of suction, while the point for  $S_{r0}=0.85$  (TX1) is on the flatter part of the curve, so a variation in  $S_r$  causes a quasi-constant value of suction according to the model, as also confirmed by the  $S_r$ -s and  $E_w$ -s paths reported in Fig. 3f.



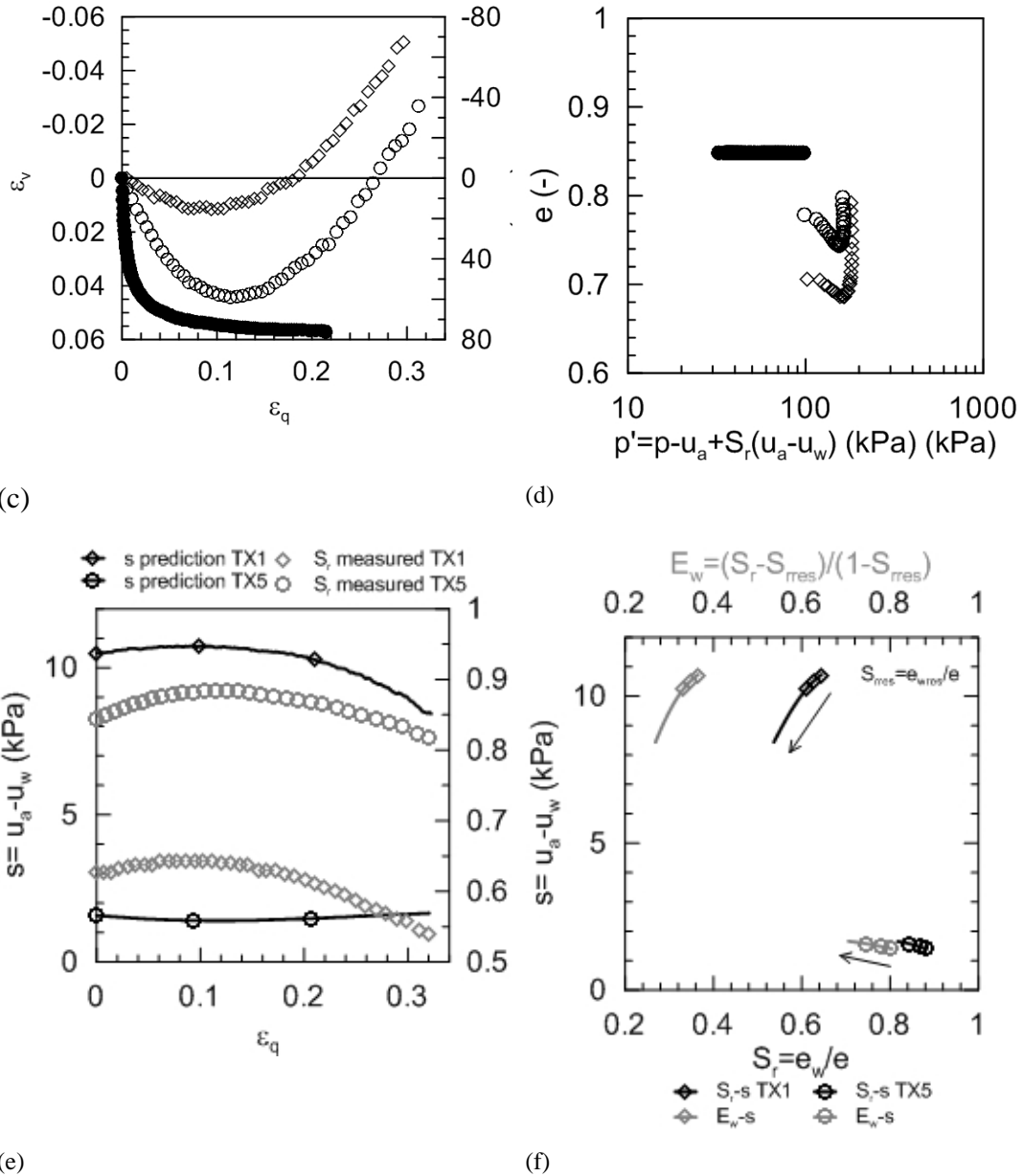


Figure 3. Triaxial compression (after consolidation to  $p'_c=100\text{kPa}$ ) under controlled axial displacement rate of  $5 \times 10^{-6} \text{ mm/s}$ : (a)  $\varepsilon_q$ - $q$  plane ; (b)  $p'$ - $q$  plane ; (c)  $\varepsilon_q$ - $\varepsilon_v$  (TX1, TX5) and  $\varepsilon_q$ - $\Delta u$  (TX9); (d)  $\log p'$ - $e$  plane; (e)  $S_r$  and  $s$  evolution with  $\varepsilon_q$ ; (f)  $S_r$ - $s$  and  $E_w$ - $s$ .

The instability induced by decreasing mean skeleton stress has been explored through calculation of the second order work. Hill's criterion captures conditional stability in these specimens for the different stress paths followed rather than a properly unstable response. Temporary instability occurs due to decreasing the effective stress for the majority of the specimens tested. The results are interpreted using the framework adopted by Chu *et al* (2003) extended to unsaturated conditions (see Figure 4). The inclination of the potential instability line  $\eta_{IL}$  can either be steeper than the critical

state line or not. However, it is clear that the change in void ratio links  $\eta_{IL}>M$  to dilation and  $\eta_{IL}<M$  to compression, and this is consistent also under both saturated and unsaturated conditions.

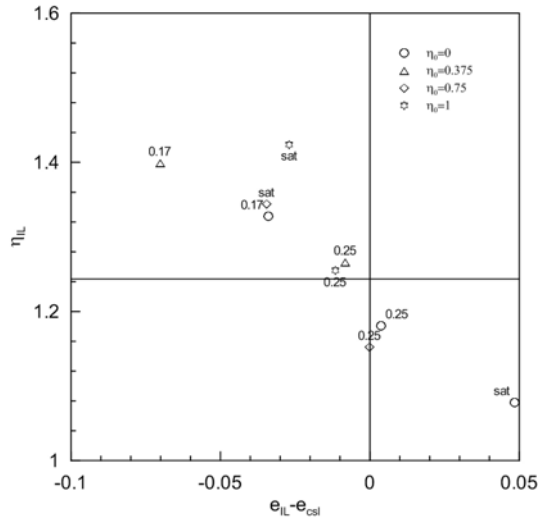


Figure 4 Potential instability line  $\eta_{IL}$  as a function of the distance  $e_{IL} - e_{csl}$ : from unsaturated to saturated condition.

## Conclusions

An extended laboratory investigation has been performed on Ruedlingen silty sand that was sampled from a steep slope where a landslide triggering experiment was carried out in March 2009. The consolidation phase has been interpreted with a simple model that well predict the entire set of results. During an infiltration process, the soil element in a slope can swell or shrink. The change in void ratio induced by the wetting front, leads the slope to be unstable for obliquity higher or lower of the critical state line depending on the void ratio at the end of consolidation phase and the bonding induced by partial saturation.

## REFERENCES

- Askarinejad, A., Casini, F., Bischof, P, Beck, A, Springman S.M. 2012. Rainfall induced instabilities: a field experiment on a silty sand slope in northern Switzerland. *Italian Geotechnical Journal* 3/12: 50-71.
- Askarinejad, A., Casini, F., Kienzler, P, Springman S.M. 2011 Comparison between the in situ and laboratory Water Retention Curves for a silty sand. *Unsaturated Soils - Proceedings of the 5<sup>th</sup> International Conference on Unsaturated Soils*, 6-8 September 2010, Barcelona, Spain: 423-428.
- Casini F. 2012. Deformation induced by wetting: a simple model. *Canadian Geotechnical Journal* 2012, 49(8): 954-960.
- Casini F., Jommi C., Springman S.M. 2010. A laboratory investigation on an undisturbed silty sand from a slope prone to landsliding. *Granular Matter* 12(3): 303-316.

- Casini F., Serri V., Springman S.M. 2012. Hydromechanical behaviour of a silty sand from a steep slope triggered by artificial rainfall: from unsaturated to saturated conditions. *Canadian Geotechnical Journal* 2013, 50(1): 28-40.
- Chu, J., Leroueil, S., Leong, W.K. 2003. Unstable behaviour of sand and its implication for slope instability. *Canadian Geotechnical Journal*. **40**, 873–885.
- Hill, R. 1958. A general theory of uniqueness and stability in elastoplastic solids. *Journal of the Mechanics and Physics of Solids* **6**: 236-249.
- Springman, S.M., Askarinejad, A., Casini, F., Friedel, S., Kienzler, P., Teysseire, P., Thielen, A. 2012. Lessons learnt from field tests in some potentially unstable slopes in switzerland. *Acta Geotechnica Slovenica* 2012/1: 5-29.